Cancer Science
The official journal of the Japanese Cancer Association

Enhanced antitumor efficacy of folate-linked liposomal doxorubicin with TGF-β type I receptor inhibitor

Yukimi Taniguchi,[1] Kumi Kawano,[1] Takuya Minowa,[1] Takashi Sugino,[2] Yuki Shimojo[1] and Yoshie Maitani[1,3]

[1]Institute of Medicinal Chemistry, Hoshi University, Tokyo; [2]Department of Basic Pathology, Fukushima Medical University, Fukushima City, Japan

(Received March 18, 2010/Revised May 24, 2010/Accepted June 3, 2010/Accepted manuscript online June 14, 2010/Article first published online July 1, 2010)

Tumor cell targeting of drug carriers is a promising strategy and uses the attachment of various ligands to enhance the therapeutic potential of chemotherapy agents. Folic acid is a high-affinity ligand for folate receptor, which is a functional tumor-specific receptor. The transforming growth factor (TGF)-β type I receptor (TβR-I) inhibitor A-83-01 was expected to enhance the accumulation of nanocarriers in tumors by changing the microvascular environment. To enhance the therapeutic effect of folate-linked liposomal doxorubicin (F-SL), we co-administrated F-SL with A-83-01. Intraperitoneally injected A-83-01-induced alterations in the cancer-associated neovasculature were examined by magnetic resonance imaging (MRI) and histological analysis. The targeting efficacy of single intravenous injections of F-SL combined with A-83-01 was evaluated by measurement of the biodistribution and the antitumor effect in mice bearing murine lung carcinoma M109. A-83-01 temporarily changed the tumor vasculature around 3 h post injection. A-83-01 induced 1.7-fold higher drug accumulation of F-SL in the tumor than liposome alone at 24 h post injection. Moreover F-SL co-administrated with A-83-01 showed significantly greater antitumor activity than F-SL alone. This study shows that co-administration of TβR-I inhibitor will open a new strategy for the use of FR-targeting nanocarriers for cancer treatment. (*Cancer Sci* 2010; 101: 2207–2213)

Polyethylene glycol (PEG)-modified nanocarriers are long-lived in the circulation and accumulate passively in tumors. To enhance the selection of target cells within the tumor site, a variety of targeting ligands have been examined in tumor-targeting drug carriers. Folate receptor (FR)-α is a glycosyl phosphatidylinositol (GPI)-anchored membrane protein that is selectively overexpressed in over 90% of ovarian carcinomas[1,2] and to various extents in other epithelial cancers but is only minimally distributed in normal tissues.[3–6] Folate receptor (FR) can serve as an excellent tumor marker and as a functional tumor-specific receptor. Folic acid, a high-affinity ligand for FR, retains its receptor-binding and endocytosis properties even if it is covalently linked to a wide variety of molecules. As a result, liposomes conjugated to the folate ligand *via* a PEG spacer have been used to deliver chemotherapeutic agents, oligonucleotides, and markers to FR-bearing tumor cells.[7–10]

In our previous studies, folate-linked liposome loaded doxorubicin (DXR), which was optimized for length of the PEG spacer and folate density (F-SL), showed strong potential *in vitro* compared with non-folate-linked PEGylated liposomes (SL).[11] In addition, F-SL showed a slightly stronger antitumor effect than SL *in vivo* irrespective of high level of accumulation on the endothelial cells of tumors.[11] To reach the FR on the tumor cell surface, F-SL requires extravasation from the blood vessel into the tumor region and to pass through the interstitium space. Therefore, we considered that active targeting by folate modification could be achieved by increasing the delivery of F-SL from the endothelial cells to the tumor cell surface with FR. Antiangiogenesis effects are known to change the tumor vasculature; therefore, this technique has already been applied in combination therapy. Bevacizumab, an antivascular endothelial growth factor (anti-VEGF) antibody was developed for blocking angiogenesis, and it is used clinically with other drugs to improve the efficiency of conventional chemotherapy.

The transforming growth factor (TGF)-β type I receptor (TβR-I) inhibitor LY364947 was reported to increase the antitumor effect of an anticancer drug encapsulated in PEGylated nanocarriers by changing the microenvironment of the vasculature.[12] The roles of TGF-β in cancer biology are complex; TGF-β can suppress or promote tumor growth depending on the type of cancer. Small molecule TβR-I inhibitors have a wide variety effects. The TβR-I inhibitor A-83-01 is one of more potent inhibitors of TβR-I kinase/activin receptor-like kinase (ALK)-5 (IC_{50} = 12 nM)[13] than previously described ALK-5 inhibitors, including LY364947 (IC_{50} = 59 nM).[14] To evaluate effect of TβR-I inhibitor on tumor vasculature *in vivo*, magnetic resonance imaging (MRI) is a powerful method.[15,16] We have reported recently that A-83-01 induced alterations in colon 26 cancer-associated neovasculature in mice using MRI.[17] In this study, we used A-83-01 to enhance extravasation of F-SL from the blood vessels. To the best of our knowledge, combination therapy with TβR-I inhibitor and active targeting carriers, such as folate-linked nanocarriers, has not been reported previously, and this report is the first to examine the antitumor effect of F-SL and A-83-01 in combination therapy.

Here we evaluated the effect of A-83-01 treatment on tumor vasculature using MRI, and then we assessed the FR-targeting effect of F-SL co-administrated with A-83-01 on the biodistribution of drug and antitumor activity in mice bearing murine lung carcinoma M109.

Materials and Methods

Materials. Hydrogenated soybean phosphatidylcholine (HSPC), amino-poly (ethyleneglycol)-distearylphosphatidylethanolamine (amino-PEG_{5000}-DSPE; PEG mean molecular weight, 5000), and n-(carbonyl-methoxypolyethyleneglycol)-1, 2-distearyl-sn-glycero-3-phosphoethanolamine (PEG_{2000}-DSPE; PEG mean molecular weight, 2000) were purchased from NOF (Tokyo, Japan). Egg phosphatidyl choline (EPC) was a kind of gift from Q.P., Tokyo, Japan. Cholesterol (Ch), DXR hydrochloride, and HPLC grade acetonitrile were purchased from Wako Pure Chemical Industries (Osaka, Japan). A-83-01 (Fig. 1a) and LY364947 were purchased from Sigma-Aldrich Japan (Tokyo, Japan). Hoechst 33342 was purchased from Invitrogen (Carlsbad, CA, USA). Magnevist (Gd-DTPA) was purchased

[3]To whom correspondence should be addressed.
E-mail: yoshie@hoshi.ac.jp

doi: 10.1111/j.1349-7006.2010.01646.x

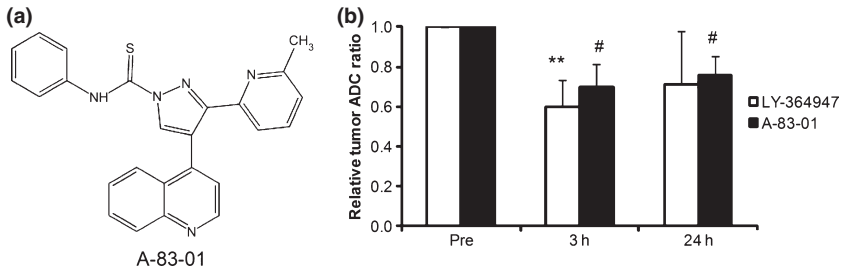

Fig. 1. Chemical structure of A-83-01 (a), and the relative apparent diffusion coefficient (ADC) ratio of M109 tumors treated with TβR-I inhibitors compared with pretreatment (Pre) (b). Three or 24 h following intraperitoneal injection of vehicle or TβR-I inhibitor (1 mg LY364947/kg or 0.5 mg A-83-01/kg), diffusion-weighted images were taken. Each value represents the mean ± SD (n = 3). $^{**}P < 0.01$ *versus* LY364947 Pre, $^{\#}P < 0.05$ *versus* A-83-01 Pre.

from Bayer-Schering Pharma (Berlin, Germany). Folate-PEG_{5000}-DSPE (F-PEG_{5000}-DSPE) was conjugated from folic acid and amino-PEG_{5000}-DSPE, which was synthesized as reported previously.[7] Other reagents used in this study were of reagent grade.

Preparation of folate-linked liposomal DXR. Liposomes were prepared from HSPC/Ch = 55/45 (mol/mol) by a dry-film method, as described previously.[11] Briefly, all lipids were dissolved in chloroform, which was removed by evaporation. The thin film was hydrated using citrate buffer (300 mM, adjusted to pH 4.0 with NaOH) at 60°C by vortex mixing and sonication. The liposomes were incubated with 2.25 mol% PEG_{2000}-DSPE and 0.25 mol% of F-PEG_{5000}-DSPE for folate-PEG-liposomes (F-SL), and incubated with 2.5 mol% PEG_{2000}-DSPE for PEGylated liposomes (SL) at 60°C for 1 h by the post-insertion technique, and then loaded with DXR by a pH gradient method.[18,19] Doxorubicin (DXR) loading efficiency was determined by separating unencapsulated from encapsulated drug using a Sephadex G-50 column. Doxorubicin (DXR) concentration was determined by measuring absorbance at 480 nm (UV-1700 Phamaspec; Shimadzu, Kyoto, Japan). The resulting mean diameter of liposomes was determined by dynamic light scattering (ELS-Z2; Otsuka Electronics, Osaka, Japan) at 25°C after diluting the liposome suspension with water.

Preparation of liposomal Gd-DTPA. Liposomal Gd-DTPA was prepared from EPC/Ch/PEG_{2000}-DSPE = 5/2/0.35 (mol/mol) (Gd-L) as described previously.[17] The average particle diameter of liposomes was adjusted to about 120 nm using ultrasound. The relaxation ratio of Gd-L was 4.48 mM/s, which was almost equal to that of Gd-DTPA (4.39 mM/s).[17]

Animals. All animal experiments were carried out in accordance with the guidelines of the Guiding Principles for the Care and Use of Laboratory Animals of Hoshi University. Murine lung carcinoma M109 cells (high FR-expressing cell line) were obtained from the Division of Chemotherapy (Translational Research Center), Chiba Cancer Center (Chiba, Japan). The cells were subcultured by employing a biogenic system of BALB/c mice. M109 cells (1.5×10^6) were inoculated subcutaneously into CDF1 female mice (5 weeks old, Sankyo Labo Service, Tokyo, Japan).

Magnetic resonance imaging (MRI). When the tumor volume reached approximately 100–200 mm^3, mice bearing M109 tumors were injected intraperitoneally with A-83-01 or LY364947, at a dose of 0.5 or 1 mg/kg, respectively, using 0.1 mg/mL dissolved in DMSO/saline = 3/2 (v/v, vehicle). Magnetic resonance imaging (MRI) was performed at 3 and 24 h post-injection of A-83-01 or LY364947, compared with pretreatment (''Pre''). Mice were anesthetized using 5% isoflurane (Abbott Japan, Tokyo, Japan) throughout the MRI experiment during their insertion into a 9.4T vertical type MRI (Varian, Palo Alto, CA, USA). High spatial resolution, two-dimensional T_2-weighted spin-echo coronal images were acquired to detect the tumor position.

Diffusion-weighted MRI was set by diffusion gradients as described previously.[17] The apparent diffusion coefficient of water in the tumors was calculated and mapped using the following parameters: repetition time (TR) = 2000 ms, echo time (TE) = 45 ms, slice thickness = 3 mm, 64×64 data matrix, axial orientation, and field-of-view = 3×3 cm^2. Three slices through the center of the tumor were acquired.

Dynamic contrast-enhanced (DCE)-MRI acquisition was applied repeatedly to acquire axial slice spoiled gradient-recalled echo images with a second temporal resolution over 6 min: TR = 7.8125 ms, TE = 2.06 ms, matrix resolution = 64×64, field of view = 3×3 cm^2, slice thickness = 4 mm, flip angle = 30°, number of slices = 1, two signal averages as described previously.[17] Gd-DTPA or Gd-L was administered at 0.1 mmol Gd/kg as a bolus with heparinized saline (total volume, ~0.4 mL). With the use of Gd-L, injected lipids containing Gd-L were retained in the tumor; therefore, different mice were used to compare pretreatment with treatment of A-83-01.

Quantitative evaluation of MRI has been described previously.[17] The apparent diffusion coefficient was obtained by the tumor regions of interest transfer to the apparent diffusion coefficient map. The concentration of Gd at each imaging time point in each voxel was obtained from conversion of pixel intensity to absolute concentration values of the contrast agent.[20] The initial area under the tumor Gd concentration-time curve (IAUGC) was calculated at 100 s post injection of contrast agent.

Immunohistochemical analysis. When the tumor volume reached approximately 100–200 mm^3, A-83-01 was intraperitoneally injected at a dose of 0.5 mg/kg. The mice were sacrificed 3 or 24 h post-injection, and each tumor was resected for A-83-01 treated mice. As a control, the mice were sacrificed 3 h post injection of vehicle, and each tumor was resected as for the untreated mice. Tumors were fixed with 10% formalin for the preparation of paraffin-embedded sections. Immunohistochemistry was performed using monoclonal antibodies against α-smooth muscle actin (Dako, Glostrup, Denmark) to identify pericyte and CD31 (BO Biosciences, San Jose, CA, USA) to detect vascular endothelial cells, in accordance with the manufacturer's protocol.

Biodistribution studies in tumor-bearing mice. When the tumor volume reached approximately 100–200 mm^3, SL or F-SL was injected intravenously at 5 mg DXR/kg with or without intraperitoneal injection of 0.5 or 1 mg A-83-01/kg. Twenty-four hours post injection of liposomes, the mice were anesthetized by ether inhalation and blood was collected and centrifuged to obtain serum. Then the anesthetized mice were sacrificed, and liver, spleen, kidney, lung, heart, and tumor tissues were collected. Doxorubicin (DXR) levels were determined

doi: 10.1111/j.1349-7006.2010.01646.x

by an HPLC method.[21] The HPLC system was composed of an LC-10AS pump (Shimadzu), a SIL-10A autoinjector (Shimadzu), an RF-10A$_{XL}$ fluorescence detector (Ex, 482 nm, Em, 550 nm; Shimadzu), and an YMC-Pack ODS-A, 150 × 4.6 mm I.D. column (YMC, Kyoto, Japan). The mobile phase was 0.1 M ammonium formate (pH 4.0): acetonitrile = 7:3 (v/v) with a flow rate of 1.0 mL/min. The concentration of DXR in each sample was determined using a calibration curve, with daunomycin as the internal standard.

Distribution of folate-linked liposomal DXR in solid tumor. When the tumor volume reached approximately 100–200 mm^3, SL or F-SL was injected intravenously at 8 mg DXR/kg with or without intraperitoneal injection of 0.5 mg A-83-01/kg, and then, 24 h post injection of liposomes, the mice were anesthetized by ether inhalation and sacrificed. For the observation of blood vessels, Hoechst 33342, which preferentially stains tumor cells adjacent to blood vessels, was injected intravenously at 7.5 mg/kg in saline 1 min before sacrifice. Tumor tissues were collected and frozen immediately in dry ice. The tumors were embedded in OCT compound and processed by frozen sectioning at 20 μm. Each frozen section was mounted on poly-L-lysine coated slides. The specimens were examined microscopically using an Eclipse TS100 microscope (Nikon, Tokyo, Japan).

Therapeutic studies. When the tumor volume reached approximately 100–200 mm^3, SL, F-SL, or free DXR was injected intravenously at 8 mg/kg, with or without intraperitoneal injection of 0.5 mg A-83-01/kg. The control group was injected intravenously with saline (0.2 mL/20 g body weight) with intraperitoneal injection of the vehicle (0.1 mL/20 g body weight). Tumor volumes and body weight were measured at regular intervals. The tumor size was measured with vernier calipers. Tumor volume was calculated using the following equation: volume = $\pi/6$ x LW^2, where L is the long diameter and W is the short diameter.

Statistical analysis. The statistical significance of the data was evaluated by analysis using Student's *t*-test. $P < 0.05$ was considered significant.

Results

Magnetic resonance imaging (MRI) of tumors treated with TβR-I inhibitors. Folate-linked liposomal doxorubicin (F-SL) and SL exhibited a high loading efficiency of >95% at a drug-to-total lipid ratio of 1:5 (w/w), which corresponded with the previous report.[11] In all cases, the average particle diameter of each liposome was ~120 nm with a narrow, monodisperse distribution. A 1 mg/kg dose of LY364947 was reported to enhance the accumulation of nanocarriers in solid tumors.[22] Because the effect of A-83-01 on M109 tumors has not been reported, we examined the tumor accumulation of SL when intraperitoneal post-injection of A-83-01 at doses of 0.5 and 1 mg/kg. Non-folate-linked PEGylated liposomal doxorubicin (SL) with A-83-01 at both doses 24 h post injection showed no significantly different DXR levels in the tumor ($P > 0.05$) (Fig. S1); therefore, we used A-83-01 at a dose of 0.5 mg/kg in the following experiments.

The effect of A-83-01 injected intraperitoneally on M109 tumor vasculature was evaluated using diffusion-weighted MRI compared with that of LY364947. The average apparent diffusion coefficient values of pretreatment (''Pre'') was 0.033 mm^2/s. The relative apparent diffusion coefficient ratio to ''Pre'' values decreased significantly at 3 h post injection of LY364947 (1 mg/kg), and 3 and 24 h post-injection of A-83-01 (0.5 mg/kg) (Fig. 1b). Because the intracellular diffusion rate is

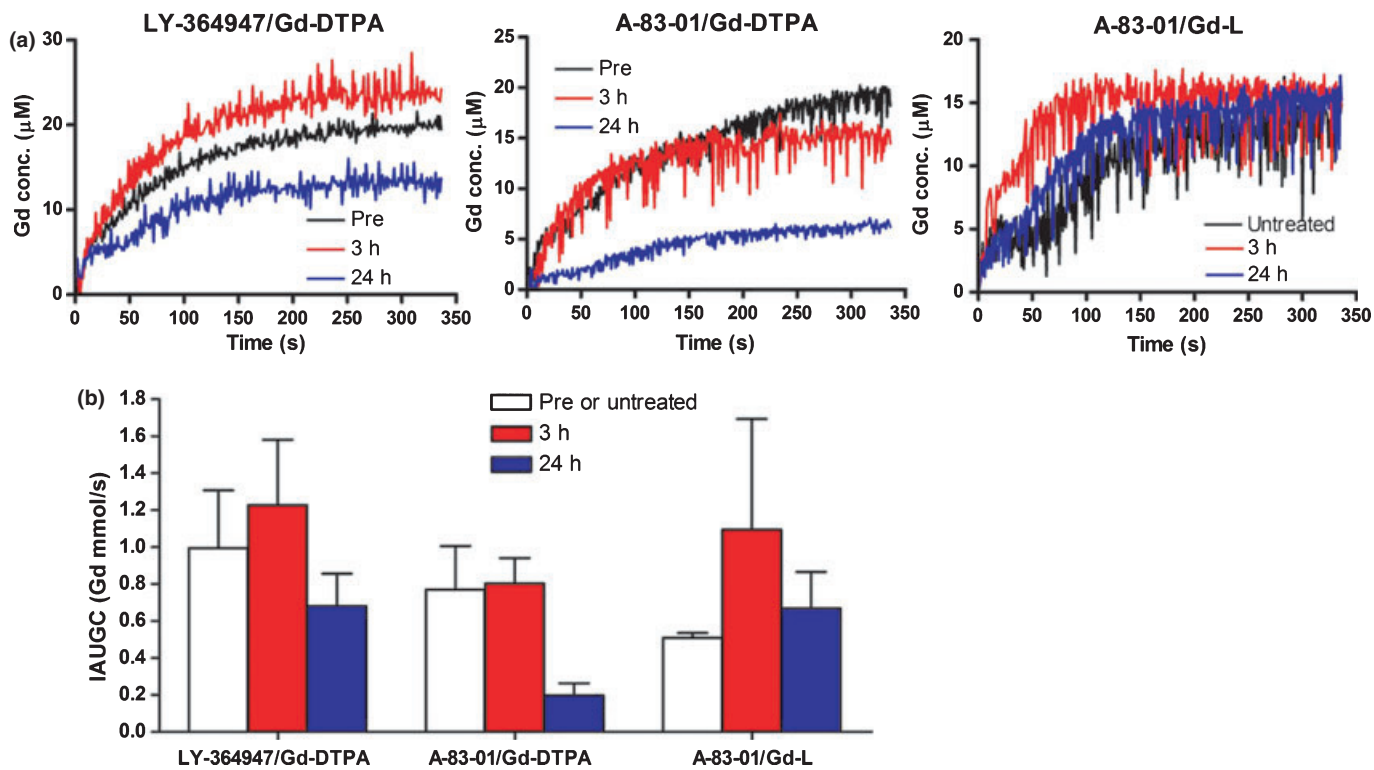

Fig. 2. Mean Gd uptake curves in the tumors before (Pre or untreated) and at different time points following intraperitoneal injection of A-83-01 or LY364947 (a), and the area under the Gd concentration curve (IAUGC) from 0 to 100 s postinjection of contrast agent (b). Three or 24 h after intraperitoneal injection of the vehicle or TβR-I inhibitor (1 mg LY364947/kg or 0.5 mg A-83-01/kg), Dynamic contrast-enhanced magnetic resonance imaging (DCE-MRI) was performed using Gd-DTPA for LY364947 and A-83-01 and Gd-L for A-83-01. Each value represents the mean ± SE ($n = 3$).

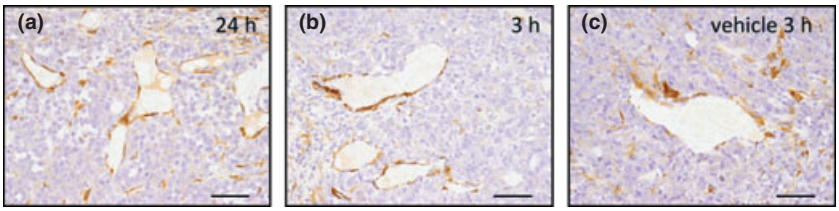

Fig. 3. Immunohistochemical analysis of pericyte association with M109 tumor vasculature following treatment with A-83-01. The pericytes lining the intratumoral blood vessels were observed in every tumor treated with A-83-01 (a,b) and vehicle (c). (a) 24 h and (b) 3 h after intraperitoneal injection of A-83-01 at a dose of 0.5 mg/kg. Bar: 50 μm.

one order smaller than that of extracellular water[23], these results suggested that A-83-01 as well as LY364947 decreased the extracellular water and/or increased intracellular water.

In DCE acquisition, a progressive accumulation of Gd-L in the tumor 3 h post injection of A-83-01 was observed during the first 100 s followed by a plateau phase (Fig. 2a). This phenomenon also appeared mice treated with LY364947 using Gd-DTPA for a contrast agent. Gd-L following A-83-01 treatment increased the IAUGC value with a wide error bar at 3 h and then decreased to a similar level to untreated controls at 24 h like Gd-DTPA following LY364947 treatment (Fig. 2b). Gd-DTPA following A-83-01 treatment did not show such an increase in the IAUGC value at 3 h as for LY364947. These results from MRI showed that A-83-01 could change the tumor microenvironment temporarily, resulting in increased IAUGC for Gd-L in the tumor. From this, we decided to co-administrate liposomal DXR with A-83-01 at the same time.

Immunohistochemical analysis of tumor vasculature treated with A-83-01. It was reported that TβR-I inhibitor treatment modified the pericyte caverage of tumor neovasculature and influenced on the tumor accumulation of nanocarriers.[12,17] Here, we evaluated the influence of A-83-01 on pericyte association with the tumor neovasculature. The pericyte lining was well conserved in tumors with and without A-83-01, except with scant pericyte association at the periphery in both tumors (Fig. 3). The vasculature-associated pericytes in the treatment group were likely to be slightly more abundant than those of the control (data not shown). These results indicated that A-83-01 did not change markedly pericyte coverage.

Biodistribution of liposomal DXR with A-83-01. We examined the influence of A-83-01 on the biodistribution of DXR in mice bearing M109 tumors at 24 h post injection of A-83-01 and liposomal formulations. As shown in Figure 4, in each organ, except in the spleen, serum, and tumor, every group showed similar DXR levels with or without A-83-01. In the spleen, SL with A-83-01 or either F-SL alone or with A-83-01 showed significantly lower DXR levels than SL alone ($P < 0.05$). Similar to the DXR level in the spleen post-injection of SL, A-83-01 greatly decreased the Gd level in the spleen post injection of lipid-nanoparticle containing Gd (Fig. S2). However, the mechanism involved was not clear. In the tumor, SL or F-SL with A-83-01 induced 1.5- or 1.7-fold higher DXR levels, respectively, than that for the liposome alone. Folate-linked liposomal doxorubicin (F-SL) with or without A-83-01 showed significantly higher DXR levels in the tumor than SL alone ($P < 0.05$). This result suggested that among the folate-linked liposomes, F-SL was more effective in tumor accumulation than SL, and A-83-01 enhanced the accumulation of liposomes only in tumors, which was likely to be due to their decrease in the spleen.

Tumor accumulation of liposomal DXR with A-83-01. Next, to evaluate the distribution of DXR around the neovasculature in tumors at 24 h following intravenous injection of liposome formulations (8 mg/kg) and intraperitoneal injection of A-83-01, we observed the staining of vessels with Hoechst 33342 using a fluorescence microscope (Fig. 5). Corresponding to the result of the tumor accumulation of DXR in Figure 4, SL or F-SL with A-83-01 showed higher DXR accumulation close to tumor vessels than that for the liposome formulations alone. This result also indicated that A-83-01 enhanced the accumulation of liposomal DXR in tumor vessels as well as in the tumor.

Antitumor effect of liposomal DXR with A-83-01. The antitumor effect of F-SL with A-83-01 was evaluated in mice bearing M109 cells. As shown in Figure 6(a), the liposomal DXR injected group showed a strong antitumor effect in comparison with saline with or without A-83-01 and free DXR treated groups. A-83-01 alone did not show an antitumor effect. In the enlargement of the liposomal DXR injected group as shown in Figure 6(b), F-SL with A-83-01 showed a significantly stronger

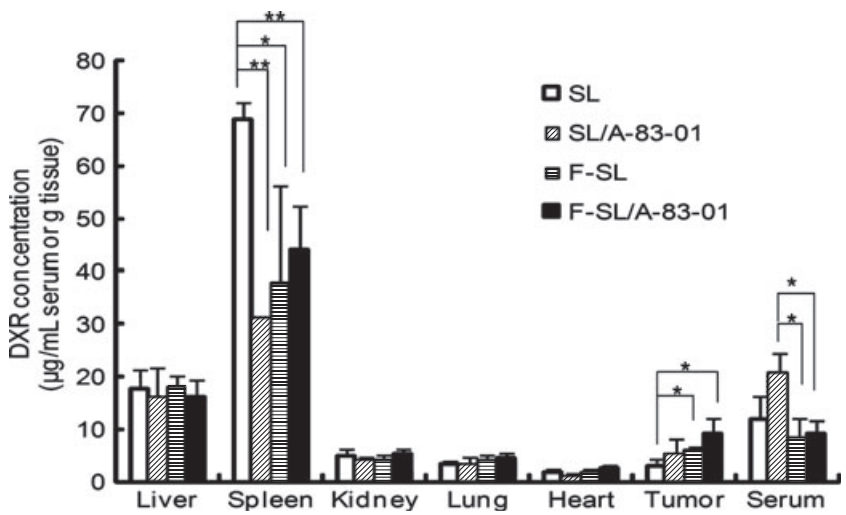

Fig. 4. Biodistribution of doxorubicin (DXR) at 24 h after intravenous injection of liposomal DXR (5 mg DXR/kg) with or without intraperitoneal injection of A-83-01 (0.5 mg A-83-01/kg) into CDF1 mice bearing M109 tumors. Each value represents the mean ± SD. ($n = 3$). $^{**}P < 0.01$, $^{*}P < 0.05$.

doi: 10.1111/j.1349-7006.2010.01646.x

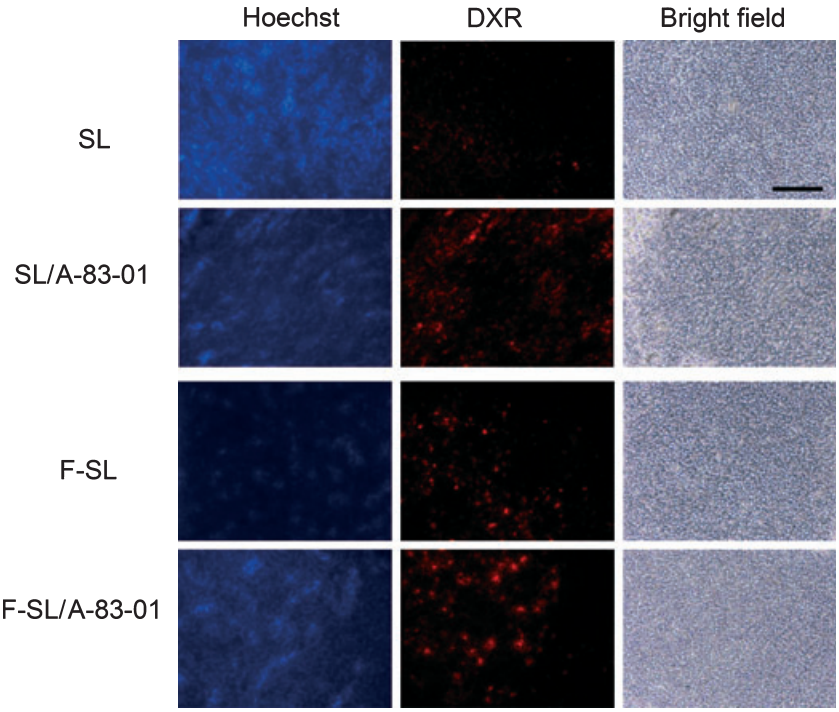

Fig. 5. Tumor accumulation of doxorubicin (DXR) in M109 tumors at 24 h after intravenous administration of liposomal DXR at a dose of 8 mg DXR/kg with or without intraperitoneal injection of A-83-01 at a dose of 0.5 mg/kg. Hoechst 33342 was injected into the tail vein 1 min before sacrifice. Then, frozen 20-μm sections were examined by fluorescence microscopy. Bar: 200 μm.

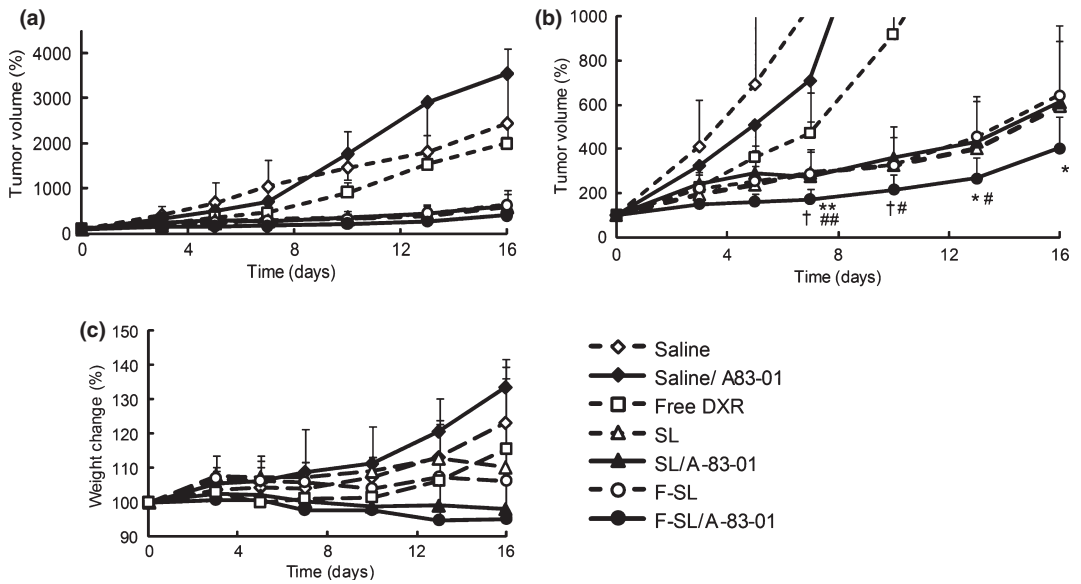

Fig. 6. Effects of A-83-01 on the antitumor activity of a single injection of liposomal doxorubicin (DXR) in CDF1 mice bearing M109 tumors. Free DXR, liposomal DXR (8 mg/kg), or saline was administered intravenously in a single bolus with or without intraperitoneal A-83-01 injection (0.5 mg/kg) to mice (n = 6–8). (a) Tumor size; (b) enlargement of (a). (c) Body weight change after drug administration. The formulations used were saline (◇), saline/A-83-01 (♦), free DXR (□), non-folate-linked PEGylated liposomal doxorubicin (SL) (△), SL/A-83-01 (▲), folate-linked liposomal doxorubicin (F-SL) (○), F-SL/A-83-01 (●). #$P < 0.05$, ##$P < 0.01$ *versus* SL, †$P < 0.05$ *versus* SL/A-83-01, *$P < 0.05$, **$P < 0.01$ *versus* F-SL. Each value represents the mean ± SD.

antitumor effect than F-SL alone on day 7 ($P < 0.01$) and days 13 and 16 ($P < 0.05$), SL alone on day 7 ($P < 0.01$) and days 10 and 13 ($P < 0.05$), or SL with A-83-01 on days 7 and 10 ($P < 0.05$). On the other hand, SL with A-83-01 showed a similar antitumor effect to SL or F-SL alone on day 16 ($P > 0.05$). As a result of observation of side-effects of DXR, a tendency of weight loss was not seen post injection of free DXR or liposomal DXR with or without A-83-01 (Fig. 6c). In addition, conspicuous side effects such as diarrhea were not observed in any groups.

Discussion

In the present study, we demonstrated that A-83-01 enhanced the antitumor effect of F-SL compared with that of F-SL alone in mice bearing M109 tumors. This finding was supported in that A-83-01 induced a temporary high leakiness of Gd-L from the tumor vasculature by means of diffusion-weighted and DCE-MRI, and enhanced the accumulation of liposomal DXR only in tumors.

Here, using liposome-entrapped Gd-DTPA, Gd-L, we could evaluate not only the effect of A-83-01[24] but also estimate the kinetics of liposomal DXR in tumors in combination therapy with A-83-01. Increased IAUGC at 3 h post injection of A-83-01 was inversely related to the apparent diffusion coefficient. These results from MRI showed that A-83-01 could change the tumor microenvironment temporarily, resulting in increased IAUGC of Gd-L in the tumor.

Next, we assessed the FR-targeting effect of F-SL with A-83-01 on the biodistribution of drug and antitumor activity in mice bearing M109 tumors. Under co-administration of A-83-01, F-SL significantly increased the antitumor effect compared with SL on days 7 and 10, whereas F-SL showed slightly higher 24-h accumulation of DXR in the tumor region than SL (Fig. 4). One of the reasons is that the accumulation of F-SL in the tumor may be faster than SL because F-SL exhibited faster clearance compared to SL.[11] In this study, since A-83-01 and liposomal DXR were injected at the same time, A-83-01 will work with early accumulated liposomes in tumors, F-SL more effectively than SL.

Compared with the result of A-83-01 treatment of colon 26 tumors in the previous study[17], the M109 tumor vasculature was more associated with pericytes; therefore, there was no observation of an increase in pericytes 24 h following A-83-01 treatment. In addition, the dose of A-83-01 was decreased from 1 to 0.5 mg/kg because toxicity was increased following injection of DXR. Even in the different tumors and at different doses, A-83-01 increased IAUGC around 3 h post injection and decreased the apparent diffusion coefficient, indicating high levels of Gd permeation from the tumor vasculature to the extracellular space. Tumor angiogenesis is a complex process and dependent on the type of tumors [22], and treatment with TβR-I inhibitor requires a regimen based on the appropriate duration of action. Further optimization of dose and injection time of A-83-01 in combination therapy with folate-linked liposomal anticancer drugs will be needed through evaluation of the microvasculature in tumors using guidance from MRI.

The present results showed that A-83-01 enhanced the accumulation of liposomal DXR only in tumors and showed a significantly stronger antitumor effect of F-SL than of F-SL alone. Further study to optimize the administration schedule of TβR-I inhibitor and F-SL will improve the FR-targeting effect of F-SL.

Acknowledgments

This work was supported in part by a grant for research on Regulatory Science of Pharmaceuticals and Medical Devices from the Ministry of Health, Labor and Welfare of Japan and by the Open Research Center Project.

References

1 Weitman SD, Lark RH, Coney LR *et al.* Distribution of the folate receptor GP38 in normal and malignant cell lines and tissues. *Cancer Res* 1992; **52**: 3396–401.
2 Elnakat H, Ratnam M. Distribution functionality and gene regulation of folate receptor isoforms: implications in targeted therapy. *Adv Drug Deliv Rev* 2004; **56**: 1067–84.
3 Wang H, Ross JF, Ratnam M. Structure and regulation of a polymorphic gene encoding folate receptor type gamma/gamma. *Nucleic Acids Res* 1998; **26**: 2132–42.
4 Ross JF, Wang H, Behm FG *et al.* Folate receptor type beta is a neutrophilic lineage marker and is differentially expressed in myeloid leukemia. *Cancer* 1999; **85**: 348–57.
5 Wu M, Gunning W, Ratnam M. Expression of folate receptor type alpha in relation to cell type, malignancy, and differentiation in ovary, uterus, and cervix. *Cancer Epidemiol Biomarkers Prev* 1999; **8**: 775–82.
6 Shen F, Ross JF, Wang X, Ratnam M. Identification of a novel folate receptor, a truncated receptor, and receptor type beta in hematopoietic cells: cDNA cloning, expression, immunoreactivity, and tissue specificity. *Biochemistry* 1994; **33**: 1209–15.
7 Gabizon A, Horowitz AT, Goren D *et al.* Targeting folate receptor with folate linked to extremities of poly(ethylene glycol)-grafted liposomes: *in vitro* studies. *Bioconjug Chem* 1999; **10**: 289–98.
8 Gabizon A, Horowitz AT, Goren D, Tzemach D, Shmeeda H, Zalipsky S. *In vivo* fate of folate-targeted polyethylene-glycol liposomes in tumor-bearing mice. *Clin Cancer Res* 2003; **9**: 6551–9.
9 Pan XQ, Wang H, Lee RJ. Antitumor activity of folate receptor-targeted liposomal doxorubicin in a KB oral carcinoma murine xenograft model. *Pharm Res* 2003; **20**: 417–22.
10 Zhao XB, Lee RJ. Tumor-selective targeted delivery of genes and antisense oligodeoxyribonucleotides via the folate receptor. *Adv Drug Deliv Rev* 2004; **56**: 1193–204.
11 Yamada A, Taniguchi Y, Kawano K, Honda T, Hattori Y, Maitani Y. Design of folate-linked liposomal Doxorubicin to its antitumor effect in mice. *Clin Cancer Res* 2008; **14**: 8161–8.
12 Kano MR, Bae Y, Iwata C *et al.* Improvement of cancer-targeting therapy, using nanocarriers for intractable solid tumors by inhibition of TGF-beta signaling. *Proc Natl Acad Sci USA* 2007; **104**: 3460–5.
13 Tojo M, Hamashima Y, Hanyu A *et al.* The ALK-5 inhibitor A-83-01 inhibits Smad signaling and epithelial-to-mesenchymal transition by transforming growth factor-beta. *Cancer Sci* 2005; **96**: 791–800.
14 Li HY, Wang Y, Heap CR *et al.* Dihydropyrrolopyrazole transforming growth factor-beta type I receptor kinase domain inhibitors: a novel benzimidazole series with selectivity versus transforming growth factor-beta type II receptor kinase and mixed lineage kinase-7. *J Med Chem* 2006; **49**: 2138–42.
15 Tsekos NV, Zhang F, Merkle H, Nagayama M, Iadecola C, Kim SG. Quantitative measurements of cerebral blood flow in rats using the FAIR technique: correlation with previous iodoantipyrine autoradiographic studies. *Magn Reson Med* 1998; **39**: 564–73.
16 O'Connor JP, Jackson A, Parker GJ, Jayson GC. DCE-MRI biomarkers in the clinical evaluation of antiangiogenic and vascular disrupting agents. *Br J Cancer* 2007; **96**: 189–95.
17 Minowa T, Kawano K, Kuribayasi H *et al.* Changes in tumor microenvironment following TGF-beta type I receptor inhibitor treatment observed by diffusion and dynamic contrast-enhanced magnetic resonance imaging. *Br J Cancer* 2009; **101**: 1884–90.
18 Uster PS, Allen TM, Daniel BE, Mendez CJ, Newman MS, Zhu GZ. Insertion of poly(ethylene glycol) derivatized phospholipid into pre-formed liposomes results in prolonged in vivo circulation time. *FEBS Lett* 1996; **386**: 243–6.
19 Lee RJ, Wang S, Turk MJ, Low PS. The effects of pH and intraliposomal buffer strength on the rate of liposome content release and intracellular drug delivery. *Biosci Rep* 1998; **18**: 69–78.
20 Bradley DP, Tessier JJ, Lacey T *et al.* Examining the acute effects of cediranib (RECENTIN, AZD2171) treatment in tumor models: a dynamic contrast-enhanced MRI study using gadopentate. *Magn Reson Imaging* 2009; **27**: 377–84.
21 Matsushita Y, Iguchi H, Kiyosaki T *et al.* A high performance liquid chromatographic method of analysis of 4′-O-tetrahydropyranyladriamycin and their metabolites in biological samples. *J Antibiot (Tokyo)* 1983; **36**: 880–6.
22 Kano MR, Komuta Y, Iwata C *et al.* Comparison of the effects of the kinase inhibitors imatinib, sorafenib, and transforming growth factor-beta receptor inhibitor on extravasation of nanoparticles from neovasculature. *Cancer Sci* 2008; **100**: 173–80.
23 Gass A, Niendorf T, Hirsch JG. Acute and chronic changes of the apparent diffusion coefficient in neurological disorders–biophysical mechanisms and possible underlying histopathology. *J Neurol Sci* 2001; **186**(Suppl 1): S15–23.
24 Turetschek K, Preda A, Novikov V *et al.* Tumor microvascular changes in antiangiogenic treatment: assessment by magnetic resonance contrast media of different molecular weights. *J Magn Reson Imaging* 2004; **20**: 138–44.

doi: 10.1111/j.1349-7006.2010.01646.x

Supporting Information

Additional supporting information may be found in the online version of this article:

Fig. S1. Tumor accumulation of doxorubicin (DXR) in CDF1 mice bearing M109 tumors at 24 h after intravenous administration of non-folate-linked PEGylated liposomal doxorubicin (SL) at a dose of 5 mg DXR/kg with or without intraperitoneal injection of A-83-01 at a dose of 0.5 or 1 mg/kg. Each value represents the mean ± SD (n = 3).

Fig. S2. Biodistribution of Gd at 24 h after intravenous injection of lipid-nanoparticle containing Gd (16.3 mg Gd/kg, NP) with or without repeated intraperitoneal injection of A-83-01 (1 mg A-83-01/kg) into CDF1 mice bearing colon 26. Each value represents the mean ± SD (n = 3).

Please note: Wiley-Blackwell are not responsible for the content or functionality of any supporting materials supplied by the authors. Any queries (other than missing material) should be directed to the corresponding author for the article.